Received: 25 May 2023 | Revised: 25 May 2023 | Accepted: 17 August 2023

DOI: 10.1002/mawe.202300146

ARTICLE

WILEY VCH

Quantitative hardness-carbon content-microstructure correlation in normalized plain carbon steel

Quantitative Korrelation zwischen Härte, Kohlenstoffgehalt und Gefüge von normalisiertem unlegiertem Stahl

J. Maity[1] | B. S. Poona[1] | M. Kumar[1] | A. Pal[1] | B. Hazra[2] | S. Sahin[1] | A. Biswas[1]

[1]Department of Metallurgical and Materials Engineering, National Institute of Technology Durgapur, Durgapur, West Bengal, India

[2]Department of Metallurgical Engineering and Materials Science, Indian Institute of Technology Bombay, Powai, Mumbai, India

Correspondence
J. Maity, Department of Metallurgical and Materials Engineering, National Institute of Technology Durgapur, Durgapur 713209, West Bengal, India.
Email: joydeep_maity@yahoo.co.in and jmaity.mme@nitdgp.ac.in

Abstract

Composition (carbon content) dependent critical structural evolution in correlation to hardness attained is judiciously investigated for plain carbon steel, the most widely used cost-effective structural material, under normalizing treatment of industrial relevance involving non-equilibrium still air cooling. The solid state phase transformation under non-equilibrium still air cooling is conceived in terms of a logarithmic variation of eutectoid carbon content with the gross carbon content of steel in view of maintaining fixed maximum solubility of carbon in α-iron with an assumption of the prevailing para-equilibrium condition. Such a unique formulation for non-equilibrium condition together with consideration of Hall–Petch type relationship and rule of mixture for two prime microconstituents (proeutectoid α-ferrite and pearlite) finally results in a new mathematical relationship for chemical composition-structure-property correlation for the non-equilibrium normalizing treatment readily practiced in industry. Indeed, a composition dependent structural refinement effect is established that is exemplified with the rise in hardness level in plain carbon steel under conventional normalizing treatment. Most importantly, the experimentally measured overall hardness values closely follow those obtained by the developed mathematical relationship, thereby meeting an ever-needed requirement of direct determination of steel hardness of practical relevance from microstructural parameters.

KEYWORDS
carbon content, hardness, mathematical correlation, microstructure, normalizing, steel

SCHLÜSSELWÖRTER
Gefüge, Härte, Kohlenstoffgehalt, mathematische Korrelation, Normalisieren, Stahl

1 | INTRODUCTION

Steel has emerged as the most widely used engineering structural material to meet techno-scientific societal need. With regard to iron-carbon phase diagram, the pro-eutectoidal and eutectoidal transformation domains primarily pertain to industrially relevant heat treatment of steels under slow cooling close to equilibrium condition. Further introspection necessitates the consideration of time-temperature-transformation diagram to realize phase evolution through solid state phase transformation under faster cooling of austenite under non-equilibrium condition. Indeed, a wide domain of microconstituents originates as the solid state phase transformation product from parent austenite phase, either in the form of single phase or mixture of many phases; namely, pro-eutectoid α-ferrite, pearlite (in lamellar form or degenerated form), bainite, martensite and so on [1–4].

Structural application essentially necessitates enhanced hardness of material often realized from refinement of the microstructural features [5]. The microstructural refinement in steel has been technologically taken up so far in view of faster cooling rate execution perspective for complete austenitization based heat treatment route [6]. Other approaches such as incomplete austenitization based heat treatment and high voltage-low current electric energy input routes have been also been tried out at laboratory scale in recent years [7–9]. In case of complete austenitization based heat treatment route, widely implemented in industry on initial trial at laboratory scale, a faster cooling rate would definitely lower down the actual transformation temperature so as to enhance the degree of undercooling. This would eventually enhance the nucleation rate to result in structural refinement [6]. Besides this basic preamble being practiced since the beginning of technological progress on steel, the effect of solute (carbon) content on structural refinement in steel even for similar cooling rate (furnace cooling pertaining to full annealing treatment) was investigated for the first time in a recent work of the present corresponding author's research group [10]. Here the shift of time-temperature-transformation diagram to the right with increasing carbon content of steel was correlated to the greater degree of undercooling for phase transformation so as to conceive structural refinement and finally ending up with development of a mathematical relationship for obtaining hardness straightway from microstructural information. However, this initial approach was taken up on annealing treatment pertaining to slow furnace cooling that eased out the difficulty in formulation of mathematical relationship for structure-property correlation via the use of Lever rule with regard to well-known iron-carbon phase diagram. However, in real industrial practice, annealing treatment is only an initial treatment to remove structural heterogeneity and internal stress; while normalizing treatment (involving non-equilibrium air cooling) is the cost-effective final heat treatment for many practically implemented steel component parts [6,11]. Realizing this eventual necessity, the present research work is formulated in studying the microstructural evolution and resultant refinement in plain carbon steel of varying solute (carbon) content up to 0.8 weight% carbon for industrially relevant normalizing process involving still air cooling with regard to carbon content-microstructure-hardness correlation perspective. The novelty of this research work stems from conceiving the solid state phase transformation under non-equilibrium still air cooling in terms of a logarithmic variation of eutectoid carbon content with the gross carbon content of steel in view of maintaining fixed maximum solubility of carbon in α-iron for para-equilibrium condition to be accounted upon. Such a new formulation for non-equilibrium condition together with a judicious analysis of experimental results (as originated from optical metallography, field emission scanning electron microscopy, electron back scattered diffraction etc.) in view of Hall–Petch type relationship and rule of mixture for two prime microconstituents (pro-eutectoid α-ferrite and pearlite) finally originates a new mathematical relationship for carbon content-microstructure-hardness correlation of the essential techno-scientific necessity.

2 | EXPERIMENTAL PROCEDURE

The plain carbon steels of hypoeutectoid category (containing 0.05 weight%, 0.192 weight%, 0.35 weight% and 0.48 weight% carbon) and eutectoid category (containing 0.79 weight% carbon) with a detailed chemical composition as enumerated in earlier work has been taken up for normalizing heat treatment process [10]. In this normalizing process, the small pieces of specimens were austenitized at 917 °C, 874 °C, 850 °C, 828 °C, 769 °C for steels containing 0.05 weight%, 0.192 weight%, 0.35 weight%, 0.48 weight% and 0.79 weight% carbon, respectively (corresponding to the fully austenitic domain) for a duration of 1 hour followed by cooling in still air to the room temperature. Besides, the temperature-time history (so called cooling curve) was recorded during still air cooling from respective austenitization temperature with the help of a K-type thermocouple connected to a digital temperature indicator, Figure 1. As indicated in the cooling curves, cooling medium being same (still air), the pathway of cooling appears to be similar for all five steel

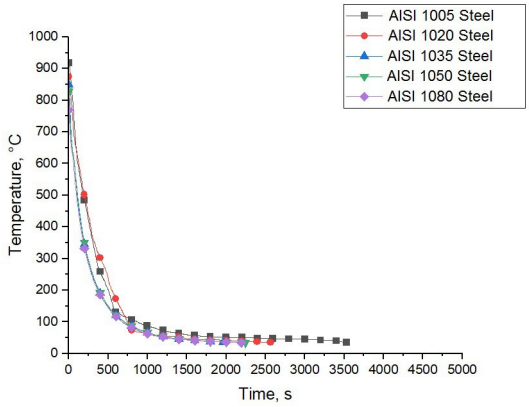

FIGURE 1 The cooling curves pertaining to still air cooling of different steels from respective austenitization temperatures.

specimens with an overall cooling rate of about $0.4^{\circ}\,C\,s^{-1}$.

All normalized steel specimens were treated with standard procedure for surface oxide and decarburized layer removal (through rough grinding up to a depth of 2 mm) followed by standard metallographic specimen preparation (fine grinding, cloth polishing and etching with Nital) as prescribed for ferrous material. The metallographic specimens prepared thereby were examined in a metallurgical optical microscope (Leica, DM 2700 M) equipped with quantitative image analysis software (LAS V4.8) and a field emission scanning electron microscope (SIGMA, Zeiss, Germany). The volume fraction of two prime microconstituents (proeutectoid α-ferrite and pearlite) and the grain size (as per ASTM E 112 standard in terms of average grain diameter, D) of the proeutectoid α-ferrite phase were determined from optical micrographs. On the other hand, the pearlite regions of the microstructures were satisfactorily resolved with field emission scanning electron microscopy and the interlamellar spacing of the pearlite (centre-to-centre distance between two adjacent cementite lamellae) was measured accordingly. Furthermore, a few selected specimens were subjected to necessary electropolishing operation using an electrolyte consisting of methyl alcohol and perchloric acid in 80:20 proportion under 14 volts of dc and thereafter taken up for electron back scattered diffraction study in respective field emission scanning electron microscope (FEI™ Quanta-3D).

Finally, the hardness values of individual prime microconstituents (proeutectoid α-ferrite and pearlite) in heat treated specimens were measured using a Vickers microhardness testing machine (MMT – X7B, Hibiki Co., Japan) at 25 gf load. Moreover, the overall Vickers hardness values of all the specimens were measured using the same hardness testing machine at 2 kgf load.

3 | RESULTS AND DISCUSSION

3.1 | Microstructure evolution in different normalized steels

The prime qualitative and quantitative interpretation is taken up with an inspection of optical micrographs of the normalized steel specimens, Figure 2a–e. Concomitant to existing knowledge-base, the two prime microconstituents in the normalized hypoeutectoid steel specimens are observed to be exhibited in the form of proeutectoid α-ferrite and pearlite, Figure 2a–d. Besides, the only microconstituent in eutectoid steel is primarily the pearlite with an apparent absence of proeutectoid α-ferrite phase, Figure 2e. Indeed, the quantification of microstructural features (mainly the prime microconstituents) as carried out onto these optical micrographs is summarized in the form of tables as well as graphical representation, Tables 1, 2, Figures 3, 4. The volume fraction of proeutectoid α-ferrite decreases and the volume fraction of pearlite increases with increase in carbon content of normalized hypoeutectoid steels. In case of extremely slow cooling (say, furnace cooling) close to equilibrium cooling, the well known 'Lever rule' provides the fraction of proeutectoid α-ferrite $\left(\frac{0.8-X}{0.8-0.025}\right)$ and the fraction of pearlite $\left(\frac{X-0.025}{0.8-0.025}\right)$ in terms of gross carbon content (X), maximum solubility of carbon in α-iron (0.025 weight%) and equilibrium eutectoid

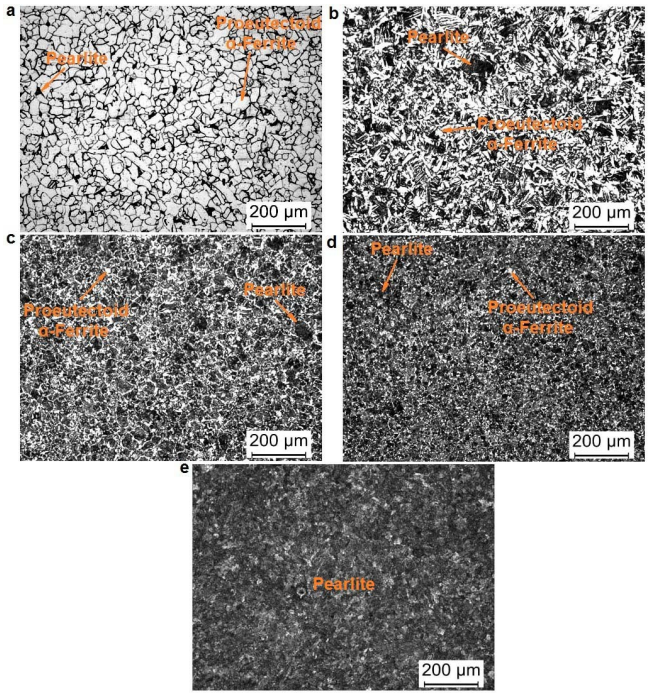

FIGURE 2 Bright field optical images of normalized steels containing (a) 0.05 wt.%C, (b) 0.192 wt.%C, (c) 0.35 wt.%C, (d) 0.48 wt.%C, and (e) 0.79 wt.%C.

TABLE 1 Relative proportion of two prime microconstituents evolved on normalizing treatment of different steels.

Steel designation	Gross carbon content (X), wt.%	Volume fraction of proeutectoid α-ferrite (f_{PF})	Volume fraction of pearlite (f_P)
AISI 1005	0.05	0.855	0.145
AISI 1020	0.192	0.653	0.347
AISI 1035	0.35	0.424	0.576
AISI 1050	0.48	0.185	0.815
AISI 1080	0.79	Negligible	1

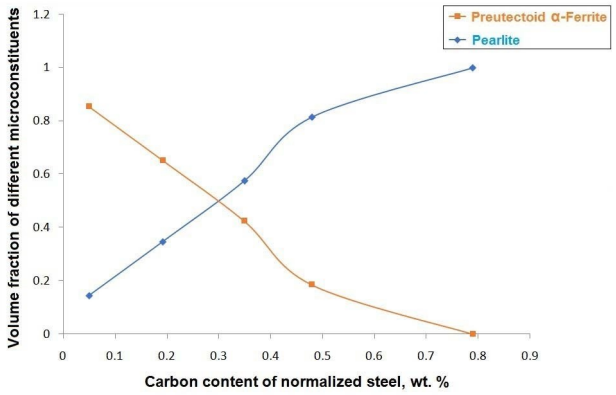

FIGURE 3 Proportion of two prime microconstituents as a function of carbon content in normalized steels.

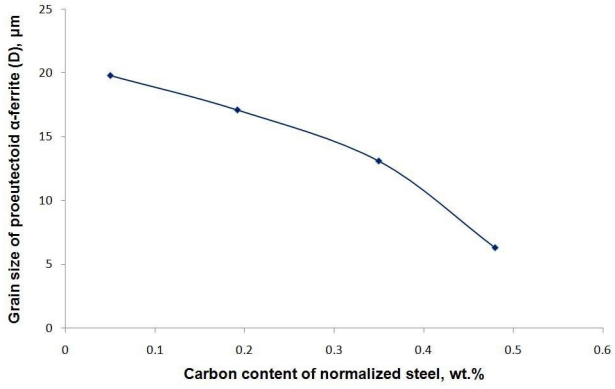

FIGURE 4 Average grain diameter of the evolved proeutectoid α-ferrite as a function of carbon content of normalized steels.

carbon content (0.8 weight%). Indeed, as per this Lever rule, the fraction of proeutectoid α-ferrite decreases and the fraction of pearlite increases with increasing carbon content (X). Theoretical calculation as per Lever rule ascertains the fraction of proeutectoid α-ferrite to be 0.968, 0.785, 0.581 and 0.413 in AISI 1005, AISI 1020, AISI 1035 and AISI 1050 steels with carbon contents of 0.05 weight%, 0.192 weight%, 0.35 weight% and 0.48 weight%, respectively. With respect to these values, the evolution of much lower fraction of proeutectoid α-ferrite in the present research work indicates toward an obvious consequence of non-equilibrium air cooling associated to the normalizing heat treatment. Fundamentally, faster cooling (as in case of normalizing) essentially results in an initiation of pearlitic transformation before necessary completion of the transformation of austenite to proeutectoid α-ferrite (as desired in slow equilibrium cooling), thereby resulting in lower proportion of proeutectoid α-ferrite and higher proportion of pearlite in the microstructure as compared to slow cooling close to equilibrium condition (say, for annealing) [6].

In view of quantitative analysis of structural features, higher carbon content eventually ascertains a lower grain size of proeutectoid α-ferrite in normalized hypoeutectoid steels, thereby representing structural refinement, Table 2. Further structural refinement of the other microconstituent is realized on analyzing the high resolution field emission scanning electron micrographs of pearlite region where the interlamellar spacing (λ) of pearlite is found to decrease with increase in gross carbon content of normalized steels, Figure 5a–e. In this regard, the detailed variation of interlamellar spacing of pearlite (measured as the centre-to-centre distance between two adjacent cementite lamellae) with carbon content in different plain carbon steels is readily analyzed and presented, Table 3, Figure 6. Indeed, the time-temperature-transformation diagram for hypoeutectoid steel is shifted to right with increasing carbon content that eventually lowers down the actual transformation temperature for a particular cooling rate (here that pertaining to still air cooling), either for the evolution of proeutectoid α-ferrite or for the evolution of pearlite [6]. This would eventually increase the respective degree of undercooling to enhance nucleation rate, thereby resulting in structural refinement so as to evolve proeutectoid α-ferrite of smaller grain size and pearlite with smaller interlamellar spacing [10].

Electron back scattered diffraction results provide further insight to the grain boundary evolution, Figure 7a–d. In case of AISI 1005 steel with greater

TABLE 2 Grain size of proeutectoid α-ferrite in different normalized steels measured in terms of average grain diameter.

Steel designation	Gross carbon content (X), wt.%	Grain size of proeutectoid α-ferrite measured as average grain diameter (D), μm
AISI 1005	0.05	19.8
AISI 1020	0.192	17.1
AISI 1035	0.35	13.1
AISI 1050	0.48	6.3
AISI 1080	0.79	Not applicable

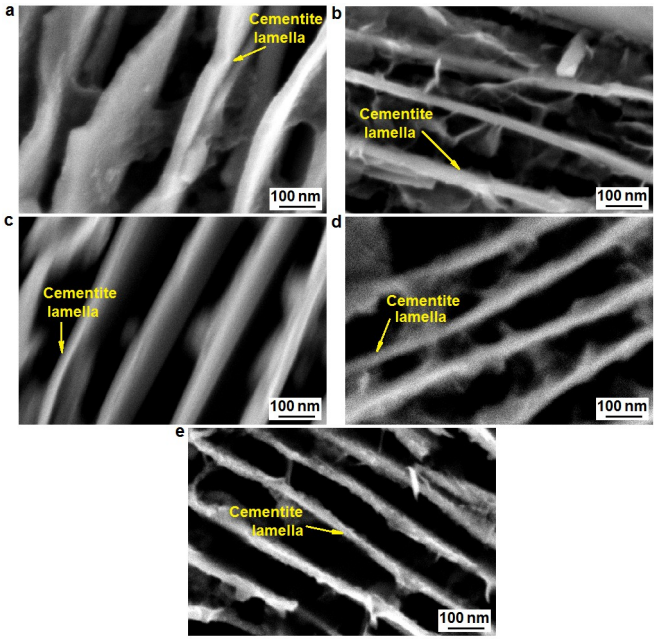

FIGURE 5 In-lens mode field emission scanning electron images corroborating pearlite region at nano-scale in normalized steels containing (a) 0.05 wt.% C, (b) 0.192 wt.% C, (c) 0.35 wt.% C, (d) 0.48 wt.% C, and (e) 0.79 wt.% C.

proportion of proeutectoid α-ferrite microconstituent, primarily the high angle grain boundaries (represented by red colour code) with large misorientation angle are present. The low angle grain boundaries are only a few, Figure 7a,b. However, for AISI 1035 steel with greater gross carbon content, more proportion of low angle grain boundaries (i.e., the subgrain boundaries) are found to originate. This is observed in terms of the corresponding colour code of low angle grain boundaries (represented with green colour) in the respective micrograph and sudden hike in relative occurrence (expressed in terms of number fraction) of low misorientation angle, Figure 7c,d. In fact, the relative proportion of pearlite is more than the proeutectoid α-ferrite in the microstructure of AISI 1035 steel. Indeed, proeutectoid α-ferrite phase evolves first as a consequence of solid state phase transformation during still air cooling from austenitization temperature. At later stage, while evolution of more proportion of pearlite, the already evolved proeutectoid α-ferrite regions are likely to experience transformation stress field all around, pearlite being the harder microconstituent. This is likely to evolve more subgrains within the proeutectoid α-ferrite region, thereby enhancing the number fraction of low misorientation angle pertaining to subgrain boundaries (low angle grain boundaries).

3.2 | Hardness of individual microconstituents

The hardness values of individual microconstituents as obtained through microhardness test at low load are readily presented in details, Table 4, Figure 8. The trend of hardness variation indicates toward an enhanced hardness of proeutectoid α-ferrite (H_{PF}) and pearlite (H_P) with increasing carbon content of normalized steel. This is essentially attributed to the reduction in grain size (D)

TABLE 3 The interlamellar spacing of pearlite as measured in different normalized steels.

Steel designation	Gross carbon content (X), wt.%	Interlamellar spacing of pearlite (λ), μm (mean ± standard deviation)
AISI 1005	0.05	0.198 ± 0.017
AISI 1020	0.192	0.181 ± 0.019
AISI 1035	0.35	0.169 ± 0.010
AISI 1050	0.48	0.137 ± 0.021
AISI 1080	0.79	0.116 ± 0.023

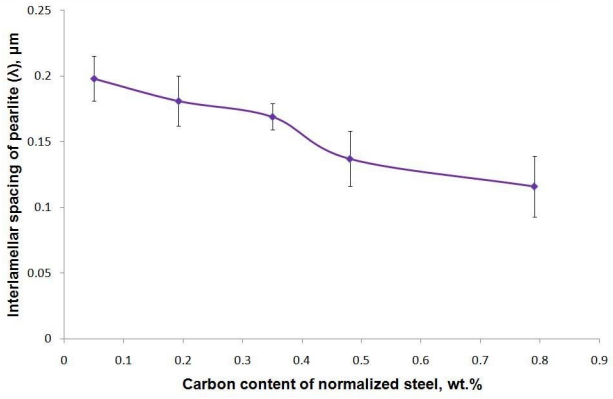

FIGURE 6 Experimentally measured interlamellar spacing of pearlite as a function of carbon content of normalized steel.

of proeutectoid α-ferrite (together with subgrain evolution) and reduction in interlamellar spacing (λ) of pearlite with increasing carbon content of normalized steel. Henceforth we need to formulate the mathematical relationship among overall hardness, gross carbon content of steel and the quantitative structural parameters (D and λ) of steel along with its validation through comparison with the experimentally measured overall hardness values.

3.3 | Mathematical formulation for overall hardness and experimental validation

Although a significant deviation from Lever rule is observed in ascertaining fraction of evolved microconstituents due to non-equilibrium air cooling pertaining to normalizing, the overall mass balance of solute (carbon) still holds good since neither any material is incorporated from outside, nor any material is lost to outside environment. Therefore, in view of the mass balance at lower critical temperature (A_1) we get:

$$f_{PF}.X_S + f_P.X_e = X \tag{1}$$

In equation (1) X_S is the maximum solubility of carbon in α-iron; X_e , the eutectoid carbon content; X, the gross carbon content of steel; f_{PF}, the fraction of proeutectoid α-ferrite, f_P, fraction of pearlite. Furthermore, the presence of two prime microconstituents in the system (proeutectoid α-ferrite and pearlite) leads to the relationship:

$$f_{PF} + f_P = 1 \tag{2}$$

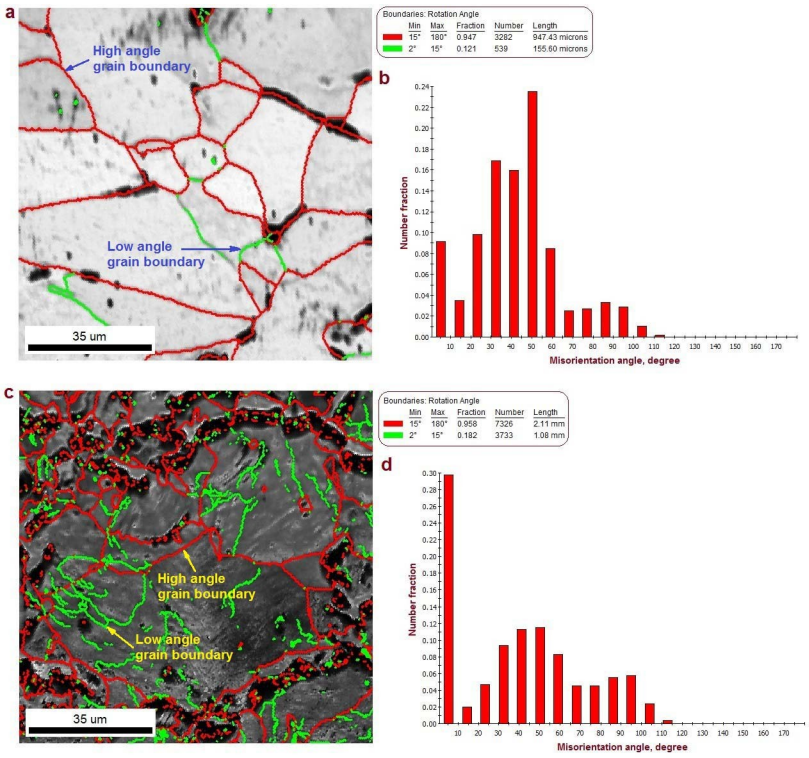

FIGURE 7 Results of electron back scattered diffraction study on selected specimens: (a) AISI 1005 steel- micrograph exhibiting grain boundary orientation and corresponding (b) misorientation angle distribution; (c) AISI 1035 steel- micrograph exhibiting grain boundary orientation and corresponding (d) misorientation angle distribution.

TABLE 4 Microhardness test results representing hardness of prime microconstituents in different normalized steels.

Steel designation	Gross carbon content (X), wt. %	Microhardness test results	
		Hardness of proeutectoid α-ferrite region (H_{PF}), HV 0.025 (mean ± standard deviation)	Hardness of pearlite region (H_P), HV 0.025 (mean ± standard deviation)
AISI 1005	0.05	144 ± 7	225 ± 9
AISI 1020	0.192	166 ± 10	249 ± 22
AISI 1035	0.35	177 ± 13	266 ± 15
AISI 1050	0.48	219 ± 12	281 ± 6
AISI 1080	0.79	Not applicable	303 ± 14

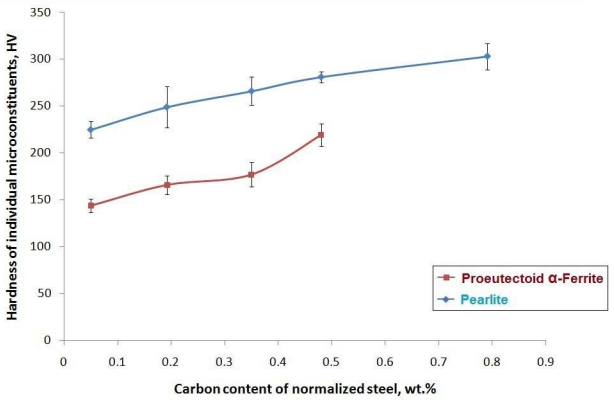

FIGURE 8 Hardness of individual microconstituents in normalized steels as a function of carbon content.

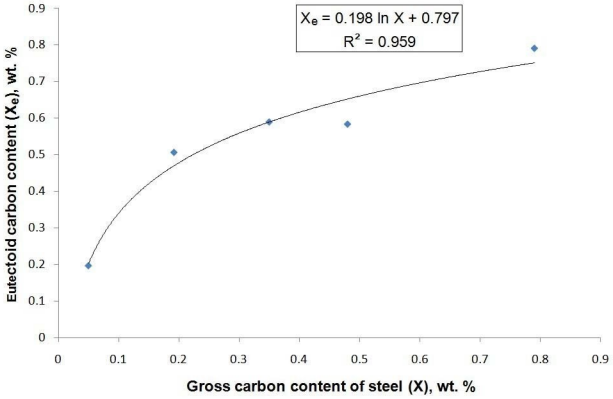

FIGURE 9 Variation of eutectoid carbon content with gross carbon content of steel.

Since as an interstitial solute carbon diffuses much faster than substitutional solutes and therefore, fundamentally the diffusion of carbon is considered not to be ceased under non-equilibrium air cooling maintaining the state of paraequilibrium [12]. In accordance, X_S may be considered as its usual fixed value of 0.025 weight % C as per Fe-C phase diagram [11]. In turn, the non-equilibrium situation will be reflected in terms of varying value of X_e with gross carbon content (X). Accordingly, putting the values of X, f_{PF} and f_P (as per the experimental result) in equation (1) we obtain the variation of eutectoid carbon content (X_e) with gross carbon content (X). This variation of X_e as a function of X is found to essentially obey a logarithmic relationship when curve fitted in Microsoft Excel Software with reasonable accuracy (coefficient of determination, $R^2 = 0.959$), Figure 9. The relationship between X_e and X obtained thereby is given as:

$$X_e = 0.198 \ln X + 0.797 \quad (3)$$

This variation under non-equilibrium condition of air cooling pertaining to normalizing eventually indicates toward a much lower value of eutectoid carbon content (X_e) at lower gross carbon content (X) of steel as compared to fixed equilibrium eutectoid carbon content of 0.8 weight %. As the gross carbon content of steel increases, the eutectoid carbon content increases toward its equilibrium value. The physical understanding of it requires a realization of solute (carbon) redistribution in concerned phases. In fact, the eutectoid carbon content envisages the carbon content of remaining austenite phase at the onset of eutectoid transformation when the proeutectoid α-ferrite phase has attained a carbon concentration of 0.025 weight % as per the maximum solubility of carbon in α-iron. In case of steel with low gross carbon content, since under non-equilibrium air cooling the relative proportion of proeutectoid α-ferrite is reduced and the proportion of remaining austenite (to be transformed to pearlite) is enhanced, the overall carbon content in relatively more proportion of remaining austenite is eventually diluted to lower down the effective value of eutectoid carbon content (X_e). Indeed, as a consequence of more availability of carbon in remaining austenite, the eutectoid carbon content increases with increase in the gross carbon content of steel concomitant to the overall mass balance.

Now, solving equation (1) and (2) we obtain:

$$f_{PF} = \frac{X_e - X}{X_e - X_S} \tag{4}$$

$$f_P = \frac{X - X_S}{X_e - X_S} \tag{5}$$

Taking $X_S = 0.025$, with regard to equations (3–5), the final expression for the fraction of proeutectoid α-ferrite and pearlite evolved in the microstructure under non-equilibrium air cooling pertaining to the normalizing treatment turns out to be:

$$f_{PF} = \frac{0.198\,ln\,X + 0.797 - X}{0.198\,ln\,X + 0.772} \tag{6}$$

$$f_P = \frac{X - 0.025}{0.198\,ln\,X + 0.772} \tag{7}$$

Now, the structure-property correlation in steel is usually expressed in terms of Hall–Petch type relationship as given below [13–15].

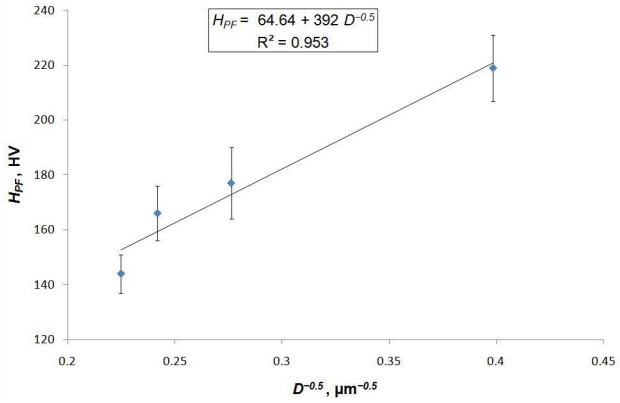

FIGURE 10 Hall–Petch type hardness variation for proeutectoid α-ferrite.

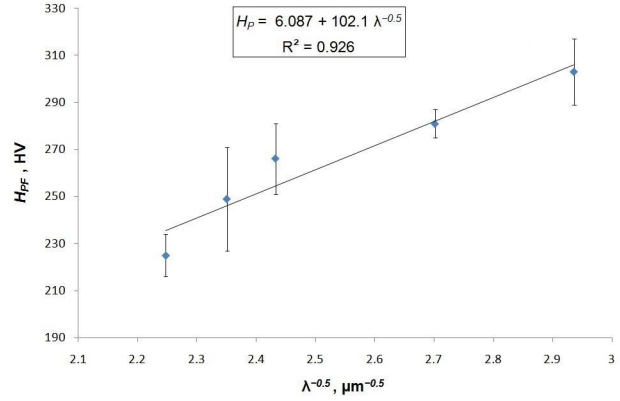

FIGURE 11 Hall–Petch type hardness variation for pearlite.

$$H_{PF} = H^0_{PF} + K_{PF} D^{-0.5} \tag{8}$$

$$H_P = H^0_P + K_P \lambda^{-0.5} \tag{9}$$

where, H°_{PF}, K_{PF}, H°_P and K_P are constants specific to the system considered. In order to find out these system specific constants so as to obtain complete mathematical relationships, H_{PF} versus $D^{-0.5}$ and H_P versus $\lambda^{-0.5}$ plots are generated and fitted to straight line with reasonable accuracy (coefficient of determination, $R^2 > 0.9$) using Microsoft Excel Software, Figures 10, 11. The resultant final empirical relationships are enumerated below.

$$H_{PF} = 64.64 + 392 D^{-0.5} \tag{10}$$

$$H_P = 6.087 + 102.1 \lambda^{-0.5} \tag{11}$$

where, D and λ are in μm; while H_{PF} and H_P are the Vickers hardness values (in kg mm^{-2}).

It is interesting to note that the slope of Hall–Petch type relationship (K_{PF}) in the present investigation (involving non-equilibrium still air cooling pertaining to normalizing treatment) for hardness variation in proeutectoid α-ferrite region is 392 HV μm$^{-1/2}$ (as per equation (10)). This value is much higher than the K_{PF} value (238 HV μm$^{-1/2}$) obtained for the annealing treatment involving slow furnace cooling in the earlier investigation by the research group of present corresponding author [10]. Such an augmented hardening effect of the proeutectoid α-ferrite region in the present work can be eventually correlated to the evolution of more proportion of subgrains within proeutectoid α-ferrite region under transformation stress exerted during evolution of greater proportion of pearlite region all around for higher gross carbon content under faster rate of cooling (air cooling) of steel as already exemplified with electron back scattered diffraction study, Figure 7.

Now, the cumulative effect of hardness values of individual microconstituents on overall hardness (H) of normalized steel may be conceived in terms of rule of mixture as given below [16].

$$H = f_{PF} H_{PF} + f_P H_P \tag{12}$$

Therefore, with regard to equation (4), (5), (10), (11) and (12) we get:

$$H = \left(\frac{0.198\,ln\,X + 0.797 - X}{0.198\,ln\,X + 0.772}\right)(64.64 + 392 D^{-0.5}) + \left(\frac{X - 0.025}{0.198\,ln\,X + 0.772}\right)(6.087 + 102.1 \lambda^{-0.5})$$

$$H = \frac{[51.366 - 58.553X + 12.799\ln X + (312.424 - 392X + 77.616\ln X)D^{-0.5} + (102.1X - 2.553)\lambda^{-0.5}]}{0.198\ln X + 0.772} \quad (13)$$

This equation (13) is the final mathematical relationship developed for the overall Vickers hardness (H) of normalized hypoeutectoid plain carbon steels in correlation to chemistry (X, the gross weight% carbon present in steel) and microstructure (D, the average grain diameter of proeutectoid α-ferrite phase in μm and λ, interlamellar spacing of pearlite in μm). In case of normalized eutectoid steel (AISI 1080 steel), since $f_{PF}=0$ and $f_P=1$, H eventually becomes equal to H_P, which is directly obtained from equation (11).

In order to justify the developed mathematical relationship, overall hardness values of all steel specimens have been measured in the same hardness testing machine at the highest load available (2 kgf) in comparison with the hardness values calculated by the developed relationship (equation (13) for hypoeutectoid steels and equation (11) for eutectoid steel), Table 5, Figure 12.

Indeed, the overall hardness increases with increase in carbon content of normalized plain carbon steel due to associated structural refinement (reduction in D and λ) even though the cooling condition remaining similar in still air. Moreover, the hardness values obtained from the developed relationship (equation (13)) closely follow the experimentally obtained overall hardness values with very small deviation (% deviation $\ll$10). This justifies the significance of the developed mathematical relationship (equation (13)) which is formulated for the first time to meet the necessity of structure-property correlation under industrially relevant normalizing treatment involving non-equilibrium air cooling.

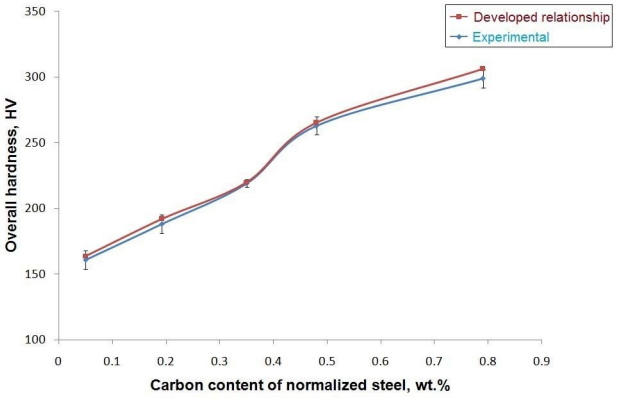

FIGURE 12 Overall hardness values in comparison with that ascertained through the developed mathematical relationship.

4 | CONCLUSIONS

1. In case of similar condition of non-equilibrium cooling (still air cooling) pertaining to the normalizing treatment of industrial process development relevance, microstructural modifications of individual microconstituents are feasible with varying chemistry (carbon content) of plain carbon steel.
2. The solid state phase transformation under non-equilibrium still air cooling is conceived in terms of variation of eutectoid carbon content with the gross carbon content of steel in view of maintaining fixed maximum solubility of carbon in α-iron with an assumption of the paraequilibrium condition to be followed.
3. Structural refinement of both the prime microconstituents (proeutectoid α-ferrite and pearlite) is found to be augmented with increasing carbon content of normalized steels till eutectoid composition.
4. A typical Hall–Petch type relationship is followed by the hardness-microconstituent size relationship both in terms of the grain size of proeutectoid α-ferrite and the interlamellar spacing of pearlite.

TABLE 5 Experimentally measured overall hardness of different normalized steels with respect to that obtained from developed mathematical relationship.

Steel designation	Gross carbon content (X), wt.%	Experimentally measured overall hardness (H_{ex}), HV 2 (mean ± standard deviation)	Overall hardness as obtained from developed mathematical relationship (H), HV	% deviation with respect to experimental overall hardness $\left(\left\|\frac{H_{ex}-H}{H_{ex}}\right\|\times 100\right)$
AISI 1005	0.05	161 ± 7	164	1.86
AISI 1020	0.192	188 ± 7	192	2.13
AISI 1035	0.35	219 ± 3	220	0.46
AISI 1050	0.48	263 ± 7	265	0.76
AISI 1080	0.79	299 ± 7	306	2.34

5. An augmented hardness enhancement effect of the proeutectoid α-ferrite region (as reflected in higher slope of Hall–Petch plot) in the present work (normalizing treatment) as compared to earlier work (annealing treatment) is presumably a consequence of the evolution of more proportion of subgrains within proeutectoid α-ferrite region under transformation stress exerted during evolution of greater proportion of pearlite region all around under faster rate of cooling (air cooling) of steel.
6. Invoking the rule of mixture further in combination with non-equlibrium variation of eutectoid carbon content and Hall–Petch relationship, a unique mathematical relationship is developed to correlate overall hardness, gross carbon content, grain size of proeutectoid α-ferrite and interlamellar spacing of pearlite in view of ascertaining chemical composition-structure-property correlation in normalized plain carbon steel. The developed relationship is found to closely abide by the experimental results.

ORCID

J. Maity http://orcid.org/0000-0002-3798-4205

REFERENCES

1. A. Saha, D. K. Mondal, J. Maity, *Mater. Sci. Eng. A* **2010**, *527*, 4001.
2. F. C. Hull, R. F. Mehl, *Trans. ASME* **1942**, *30*, 381.
3. H. K. D. H. Bhadeshia, D. V. Edmonds, *Acta Metall. Mater.* **1980**, *24*, 1265.
4. J. Maity, A. Sharma, *Philos. Mag.* **2023**, *103*, 407.
5. A. R. Subhani, D. K. Mondal, C. Mondal, J. Maity, *Philos. Mag. Lett.* **2018**, *98*, 240.
6. C. R. Brooks, Principle of the Heat Treatment of Plain Carbon and Low Alloy Steels, *ASM International*, Ohio, **1996**.
7. J. Maity, *Philos. Mag.* **2023**, *103*, 611.
8. M. Mallick, S. K. Mitra, D. Basak, N. K. Roy, J. Maity, *Philos. Mag.* **2021**, *101*, 555.
9. M. Mallick, S. K. Mitra, D. Basak, N. K. Roy, J. Maity, *Steel Res. Int.* **2021**, *92*, 1.
10. J. Maity, S. A. Rahman, S. Alam, K. K. Singh, P. Kumar, S. Hembram, *Materialwiss. Werkstofftech.* **2023**, *54*, 335.
11. X. Xie, Steel Heat Treatment Hand Book, in: G. E.Totten, M. A. H. Howes (Eds.), Marcel Dekker, 990–995, New York, **1997**.
12. H. K. D. H. Bhadeshia, L. E. Svensson, Mathematical Modelling of Weld Phenomena, (Ed.) H. Cerjak, K. E. Esterling, *Institute of Materials*, 109–182, London, **1993**.
13. E. O. Hall, *Proc. Phys. Soc. London Sect. B* **1951**, *64*, 747.
14. N. J. Petch, *J. Iron Steel Inst. London* **1953**, *174*, 25.
15. S. Sadeghpour, *International Journal of Iron and Steel Society of Iran* **2011**, *8*, 1.
16. M. Alibeyki, H. Mirzadeh, M. Najafi, A. Kalhor, *J. Mater. Eng. Perform.* **2017**, *26*, 2683.

How to cite this article: J. Maity, B. S. Poona, M. Kumar, A. Pal, B. Hazra, S. Sahin, A. Biswas, *Materialwiss. Werkstofftech.* **2023**, *54*, e202300146. https://doi.org/10.1002/mawe.202300146